Tran. Magn. Soc. Japan. Vol.4, No.4-2, 2004, 278-281.

Novel Magneto-optical Microscope Using Optical Modulation Technique

T. Ishibashi, Z. Kuang, Y. Konishi*, K. Akahane*, X. R. Zhao**, T. Hasegawa*** and K. Sato
Tokyo University of Agriculture and Technology, *2-24-16 Nakacho, Koganei, Tokyo 184-8588, Japan*
*Neoark Corporation, *2-8-33 Wakamatsu-cho, Fuchu, Tokyo 183-0005, Japan*
**National Institute for Materials Science, *1-1 Namiki Tsukuba, Ibaraki 305-0044, Japan*
***The University of Tokyo, *7-3-1 Hongo, Bunkyo-ku, Tokyo 113-0033, Japan*

Magneto-optical microscope utilizing polarization modulation technique was developed to obtain magneto-optical (MO) images involving quantities of MO effects, such as Faraday rotation and ellipticity. Faraday rotation images were calculated from three images taken with a linear polarized light and circularly polarized lights with left and right rotation. Square dots pattern of $Y_2BiFe_4GaO_{12}$ film with a dimension of 50μm × 50μm and a thickness of 200 nm were measured as a sample, and the magnetic contrast was clearly observed in images of both Faraday rotation and ellipticity at wavelength. The quantitative value of the Faraday rotation and the ellipticity were measured to be 0.5° and 0.15°, respectively. Resolution of the Faraday image was obtained to be less than 0.05° by taking an integration of images and a smoothing treatment.

Key words: magneto-optical microscope, polarization modulation technique, Faraday rotation image, $Y_2BiFe_4GaO_{12}$ film

1. Introduction

Magneto-optical (MO) microscopes have been used as one of the most convenient techniques for observation of magnetic domain structures in magnetic materials. However, the crossed-polarizer technique employed by most of the conventional MO microscopes do not allow a simultaneous observation of Faraday rotation θ_F and ellipticity η_F images, nor a quantitative evaluation of values of θ_F and η_F. The measurement of MO-hysteresis curves at an arbitrary position on the image is also difficult since in most cases MO image is constructed by a subtraction of images for opposite magnetic fields. In this study, we propose a novel concept of MO microscope utilizing a sort of polarization modulation technique.[1] This microscope can be applied to a variety of quantitative magnetic imaging measurements, such as the magnetic domain observation, the vortex penetration imaging in superconductors, and the local magnetic characterization in combinatorial materials. Application of this novel technique to combinatorial materials has been published elsewhere.[2]

In this paper, we describe a physical explanation of the MO imaging utilizing the polarization modulation technique, and demonstrate the imaging of Faraday rotation θ_F and Faraday ellipticity η_F.

2. MO microscope setup

Figure 1 shows a schematic drawing of the MO microscope used in this experiment. A conventional optical microscope (Olympus, BH-UMA) was employed. In order to utilize optical modulation technique in a MO microscope, a polarizer (Glan-Thompson prism; Karl Lambrecht corp., MG*B10), a quarter-wave plate (ahcromatic wave plate CVI, ACP-400-700) and an analyzer (Glan-Thompson prism; Karl Lambrecht corp., MG*B10) were installed into the conventional optical microscope. To modulate the polarization states of lights, we use a rotatable quarter-wave plate instead of the photo-elastic modulator (PEM) used in the spectroscopic measurement in ref. 1, because a CCD device does not response a modulation frequency of 50kHz by the PEM. An objective lens (Olympus, NeoSPlanNIC×10) was used in this experiment. Digital images of 1280×1024 pixels are taken by a cooled CCD camera (Hamamatsu, C4880) with a 12-bit A-D converter. A halogen tungsten lamp (20W) equipped in the microscope was used as a light source. In this experiment, an interference filter was used as a band-pass filter to select a wavelength of 500 nm.

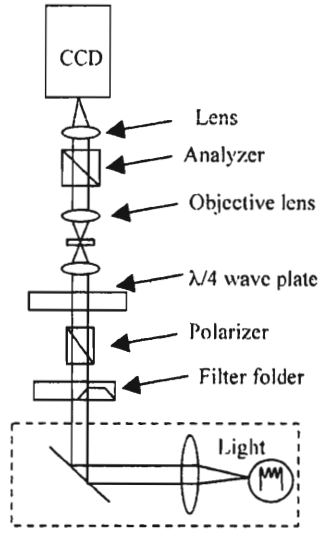

Fig.1 Magneto-optical microscope utilizing polarization modulation technique.

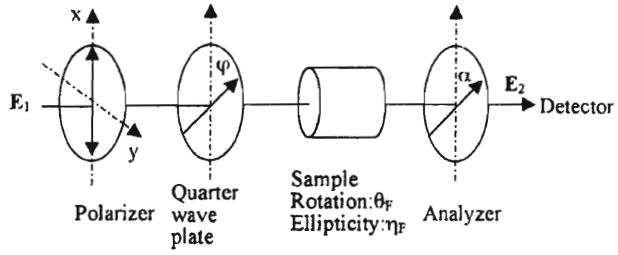

Fig.2 An optical setting for the optical modulation technique.

All the images shown in this paper were taken with an exposure time of 8 sec, and 10-times integration. Smoothing treatment was done for all the pixels, which takes an average of 9 pixels around the each pixel.

3 Theoretical back ground

A principle of the MO imaging utilizing the polarization modulation technique can be analyzed by the Jones matrix method described as follows. Each optical component shown in Fig.2 is expressed by the matrix. Assume that the polarization axis is set along the x-axis. Then the Jones matrix of the polarizer can be expressed as

$$\boldsymbol{P} = \begin{pmatrix} 1 & 0 \\ 0 & 0 \end{pmatrix}, \tag{1}$$

A quater wave plate with an optic axis at angle φ from vertical (x) axis is denoted by

$$\boldsymbol{Q} = \begin{pmatrix} 1 + i\cos 2\varphi & i\sin 2\varphi \\ i\sin 2\varphi & 1 - i\cos 2\varphi \end{pmatrix}. \tag{2}$$

A sample is expressed by

$$\boldsymbol{S} = \begin{pmatrix} \cos\theta_F + i\eta_F \sin\theta_F & -\sin\theta_F + i\eta_F \cos\theta_F \\ \sin\theta_F - i\eta_F \cos\theta_F & \cos\theta_F + i\eta_F \sin\theta_F \end{pmatrix}. \tag{3}$$

Analyzer with transmission axis α is

$$\boldsymbol{A} = \begin{pmatrix} \cos^2\alpha & \cos\alpha\sin\alpha \\ \cos\alpha\sin\alpha & \sin^2\alpha \end{pmatrix}. \tag{4}$$

For the sake of convenience, we assume $\alpha = \pi/4$, then

$$\boldsymbol{A} = \frac{1}{2}\begin{pmatrix} 1 & 1 \\ 1 & 1 \end{pmatrix}. \tag{5}$$

Output signal $\boldsymbol{E}_2$ is calculated by as follows,

$$\begin{aligned} \boldsymbol{E}_2 &= \boldsymbol{ASQPE}_1 \\ &= \frac{1}{2}\begin{pmatrix} 1 & 1 \\ 1 & 1 \end{pmatrix}\begin{pmatrix} \cos\theta_F + i\eta_F \sin\theta_F & -\sin\theta_F + i\eta_F \cos\theta_F \\ \sin\theta_F - i\eta_F \cos\theta_F & \cos\theta_F + i\eta_F \sin\theta_F \end{pmatrix}\begin{pmatrix} 1 + i\cos 2\varphi & i\sin 2\varphi \\ i\sin 2\varphi & 1 - i\cos 2\varphi \end{pmatrix}\begin{pmatrix} 1 & 0 \\ 0 & 0 \end{pmatrix}\begin{pmatrix} E_x \\ E_y \end{pmatrix} \\ &= \frac{1}{2}\begin{pmatrix} \cos\theta_F + \sin\theta_F - \eta_F(\sin(2\varphi+\theta_F) - \cos(2\varphi+\theta_F)) + i\{\cos(2\varphi+\theta_F) + \sin(2\varphi+\theta_F) + \eta_F(\sin\theta_F - \cos\theta_F)\} \\ \cos\theta_F + \sin\theta_F - \eta_F(\sin(2\varphi+\theta_F) - \cos(2\varphi+\theta_F)) + i\{\cos(2\varphi+\theta_F) + \sin(2\varphi+\theta_F) + \eta_F(\sin\theta_F - \cos\theta_F)\} \end{pmatrix} E_x, \end{aligned} \tag{6}$$

where $\boldsymbol{E}_1 = (E_x, E_y)$ is an input light. Intensity $I(\varphi)$ measured by a detector is a square of the absolute value of $\boldsymbol{E}_2$,

$$I(\varphi) = \left\{\left(\cos\theta_F + \sin\theta_F - \eta_F(\sin(2\varphi+\theta_F) - \cos(2\varphi+\theta_F))\right)^2 + \left(\cos(2\varphi+\theta_F) + \sin(2\varphi+\theta_F) + \eta_F(\sin\theta_F - \cos\theta_F)\right)^2\right\}|E_x|^2/4. \tag{7}$$

For φ=0, $+\pi/4$ and $-\pi/4$, the beam incident into the sample is linearly polarized (LP), right-circularly polarized (RCP) and left-circularly polarized (LCP), respectively. The calculated light intensities at the CCD camera normalized by a initial light intensity $I_{IN} = |\boldsymbol{E}_1|^2$ for the Faraday rotation angles θ_F = 5°, 0° and –5° are plotted in Fig. 3 as a function of the quarter-wave plate angle by solid, dashed and dotted curves respectively. Here the analyzer angle α is set at 45° and the ellipticity of the sample η_F is assumed to be 0°. As observed in the solid curve, intensities $I(0)$, $I(+\pi/4)$ and $I(-\pi/4)$ take the same value ($0.25\times I_{IN}$) in the case of no Faraday rotation; i.e., θ_F =0°. For a finite value of Faraday rotation θ_F, $I(0)$ becomes to deviate from 0.25 × I_{IN}, while $I(+\pi/4)$ and $I(-\pi/4)$ remain unchanged as shown by dashed and dotted curves. It is therefore clear that magnetic contrast images for Faraday rotation can easily be obtained by simply taking the difference $I(0)$-$I(+\pi/4)$ or $I(0)$-$I(-\pi/4)$.

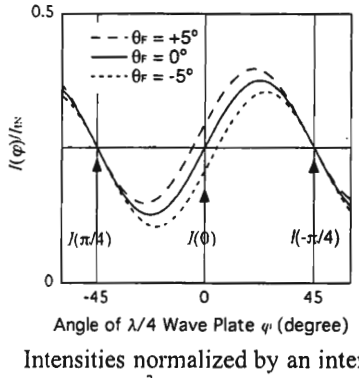

Fig. 3 Intensities normalized by an intensity of initial light $I_{IN} = |\boldsymbol{E}_1|^2$ depending on the angle of $\lambda/4$ wave plate, where $\alpha = \lambda/4$ and η_F =0.

Although this procedure is quite similar to the conventional crossed polarizer technique, an advantage of the present system is a large signal intensity of the images compared with the former. In this system, light intensities $I(0)$ and $I(+\pi/4)$ are approximately 25% of the input light intensity $I_{IN} = |E_1|^2$ if an absorption by a sample is not assumed, whereas the light intensity is no more than 1% of I_{IN} in the crossed polarizer technique. Indeed, in the latter technique the angle of the analyzer α is set at slightly off (namely around 5°) from the extinction point, which leads to a poor image intensity such as 0.76% of I_{IN} for α=5°. The brightness of images has a crucial importance for a real-time MO imaging, because the higher intensity of the image makes the exposure time short.

Another and the most important advantage of our technique is that not only a simultaneous observation of θ_F and η_F images can be taken but also a quantitative evaluation of θ_F and η_F images is possible. Theoretically, θ_F and η_F images can be calculated as follows,

$$\theta_F = \frac{1}{2} sin^{-1}\left\{\frac{2I(0) - \{I(\pi/4) + I(-\pi/4)\}}{(1-\eta_F{}^2)|E_x|^2}\right\}, \quad (8)$$

$$\eta_F = -\frac{1}{2}\{I(\pi/4) - I(-\pi/4)\}/|E_x|^2. \quad (9)$$

For small θ_F and η_F less than a few degrees, $|E_x|^2$ in the equation (8) and (9) are replaced by $\{I(+\pi/4) + I(-\pi/4)\}$ and they are simplified as follows,

$$\theta_F \approx \frac{1}{2}\left\{\frac{2I(0) - [I(\pi/4) + I(-\pi/4)]}{(1-\eta_F{}^2)[I(\pi/4) + I(-\pi/4)]}\right\}, \quad (10)$$

$$\eta_F \approx -\frac{1}{2}\left\{\frac{I(\pi/4) - I(-\pi/4)}{I(\pi/4) + I(-\pi/4)}\right\}, \quad (11)$$

Note that, for large values of θ_F and η_F, equation (10) and (11) should include large errors. For example, the error is 35% in θ_F and 22% in η_F for θ_F = 30° and η_F = 30°, while those are less than 0.1% for θ_F = 1° and η_F = 1°.

3. Experiment

A sample used in this experiment was Bi, Ga substituted yttrium Iron garnet ($Y_2BiFe_4GaO_{12}$) thin film showing a perpendicular magnetization prepared by a metal-organic decomposition method. Detailed description of the method will be published elsewhere. Since the microscope is equipped with no electromagnet in the present stage, all the measurements of this study have been carried out using samples at a remanent state. Change of the magnetic state of the sample is performed by putting the sample in a permanent magnet with B=0.5 T.

In order to investigate the resolution of the magneto-optical contrast, the garnet thin film was patterned into square dot arrays by a photo-lithography. The size of each dot is 50 μm × 50μm in area and 200 nm in thickness, and the separation is 50 μm.

Figure 4 shows images of (a) $I(0)$, (b) $I(\pi/4)$, (c) $I(-\pi/4)$, (d) Faraday rotation θ_F and (e) Faraday ellipticity η_F. Images of Figs. 4(d) and 4(e) are obtained from those of Figs. 4(a)-(c) by calculation at each pixel applying equations (10) and (11), respectively. Then images are constructed using obtained values of θ_F and η_F. It means that the images obtained in this procedure not only show magnetic contrast, but also provide the quantitative values of θ_F and η_F for all the pixels. Therefore, this imaging technique is useful not only for homogeneous samples such as thin films, but also for inhomogeneous samples as measured in this experiment. In Figs. 4(d) and 4(e), the contrast s is directly associated with values of θ_F and η_F, respectively. This is also an advantage of this technique, since the image contrast usually cannot directly connected to magnetic contrast in the inhomogeneous materials like this case where the sample consists of two portions with different transmittance, i.e., the bare glass substrate and the garnet patterns on the substrate.

Figure 5 shows Faraday rotation images of the garnet dot structure measured at the wavelength of 500 nm. Figures 5(a) and (b) were measured for opposite remanent states after magnetizing by the field of opposite directions.

The magnetic contrast between the glass and the garnet portions are obvious. In addition, a reversal of the magnetic contrast is clearly observed by a reversal of the direction of the magnetization.

The Faraday ellipticity images for opposite magnetization directions are shown in Fig. 6. These images are calculated using the same $I(0)$, $I(+\pi/4)$ and $I(-\pi/4)$ values as used for Faraday rotation images of Figs. 5(a) and 5(b). A reversal of the contrast of ellipticity images by magnetic reversal is also clearly observed.

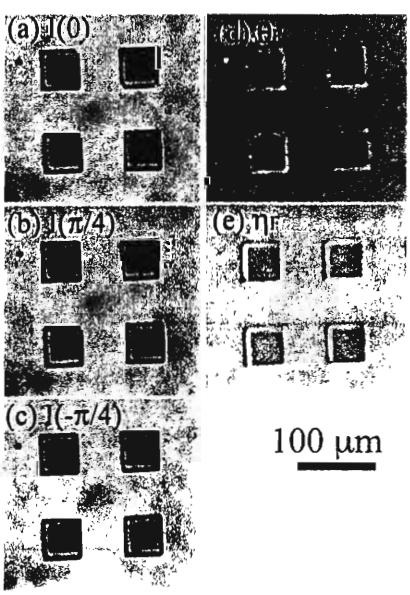

Fig.4 Images taken by CCD camera, (a)$I(0)$, (b)$I(\pi/4)$, (c)$I(\pi/4)$, and images of (d)Faraday rotation and (e)ellipticity.

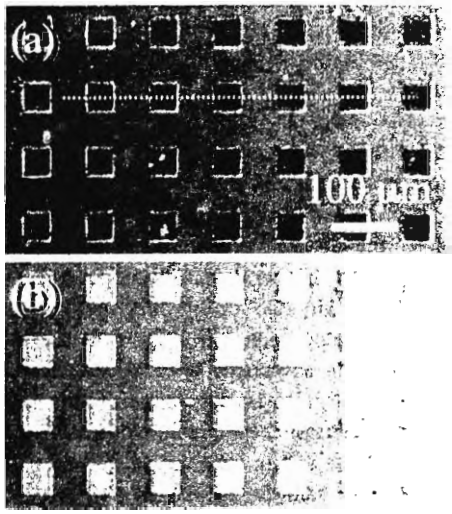

Fig.5 Images of Faraday rotation measured for opposite remanent states.

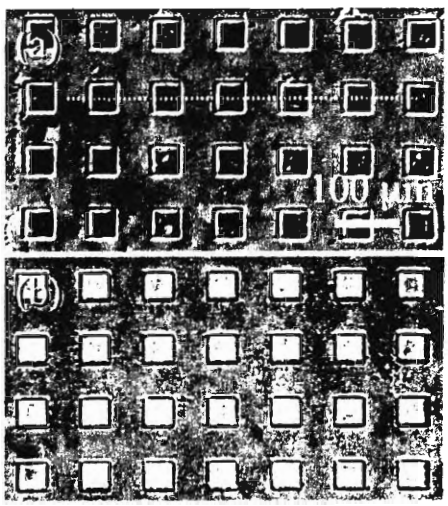

Fig.6 (a) and (b) are images of Faraday ellipticity measured simultaneously with Fig.5(a) and Fig.5(b), respectively.

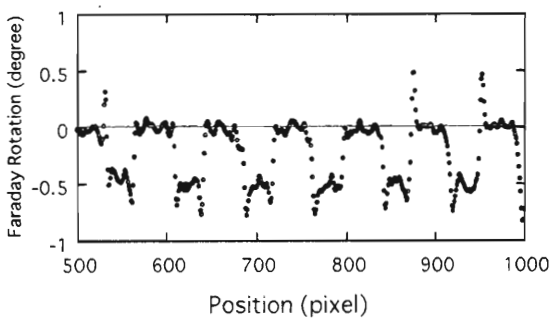

Fig. 7 Cross section of the image of Faraday rotation shown in Fig.5(a).

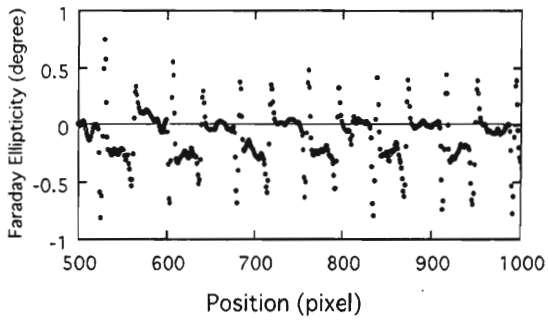

Fig. 8 Cross section of the image of Faraday ellipticity shown in Fig.6(a).

Finally, qualitative magneto-optical values are discussed. The cross sectional plots of the Faraday rotation θ_F and ellipticity η_F as indicated by doted lines in Fig.5(a) and Fig.6(a) are shown in Figs.7 and 8, respectively. The values of θ_F and η_F in the garnet dots are determined to be 0.5° and 0.3°, respectively. These values are consistent with those measured by an MO spectrometer. The minimum resolution of the Faraday rotation is estimated to be less than 0.05° by taking an integration of images and a smoothing processing. However, it is difficult to determine the spatial resolution from the present experiment because of a depolarization at the edge of dots resulting in a spike-shape noise. For this purpose, therefore, a homogeneous sample should be measured. Further improvement using a high magnifying lens is under investigation.

4. Conclusions

We have developed an MO microscope using an optical modulation technique with a rotatable quarter-wave plate. A novel MO imaging technique was described and demonstrated. Faraday rotation and ellipticity images can be constructed from three images taken with LP, LCP and RCP, obtained by using the rotatable quarter-wave plate. Clear magnetic contrasts were observed in a patterned 200nm-thick$Y_2BiFe_4GaO_{12}$ film for both Faraday rotation and ellipticity images, and those values were measured to be 0.5° and 0.3°, respectively.

Acknowledgements This work has been carried out under the 21st COE Project "Future Nano Materials" of TUAT and supported in part by the Grant-in-Aid for Scientific Research (Exploratory Research) from Japan Society for the Promotion of Science.

References

1) K. Sato, Jpn. J. Appl. Phys. **20**, 2403 (1981).
2) X. R. Zhao, N. Okazaki, Y. Konishi, K. Akahane, Z. Kuang, T. Ishibashi, K. Sato, H. Koinuma and T. Hasegawa, Appl. Surf. Sci. **223**, 73 (2004).

(Received April 19, 2004, Accepted August 9, 2004)